Tracking Control of Overhead Crane Using Output Feedback With Adaptive Unscented Kalman Filter and Condition-Based Selective Scaling

JAEHOON KIM[ID][1]**, BÁLINT KISS**[ID][2]**, (Member, IEEE), DONGGIL KIM**[ID][3]**, AND DONGIK LEE**[ID][1]**, (Member, IEEE)**

[1]School of Electronic and Electrical Engineering, Kyungpook National University, Bukgu, Daegu 41566, South Korea
[2]Department of Control Engineering and Information Technology, Budapest University of Technology and Economics, 1111 Budapest, Hungary
[3]Department of Robot Engineering, Kyungil University, Gyeongsan 38428, South Korea

Corresponding author: Dongik Lee (dilee@ee.knu.ac.kr)

ABSTRACT Most of the advanced nonlinear control strategies reported in the literature for underactuated mechanisms, such as overhead cranes, require the knowledge of all state variables. For cranes, the state vector includes variables related to the load sway and its velocity. The flatness property of crane-like systems can be exploited to solve both motion planning and tracking problems, so that the load (whose coordinates are included in the set of the flat outputs) exponentially follows a rapid reference trajectory. However, unmodeled friction phenomena and limitations on the direct measurement of sway-related state variables usually impede the practical implementation of flatness-based control laws. This paper proposes the use of an adaptive unscented Kalman filter to estimate friction forces and unmeasured state variables. The convergence of the filter is improved using a novel technique, called condition-based selective scaling. The performance of the suggested scheme is verified through a set of computer simulations on a 2D overhead crane system.

INDEX TERMS Overhead crane, feedback linearization, flatness based control, adaptive unscented Kalman filter, condition-based selective scaling.

I. INTRODUCTION

Automatic control of cranes generally aims to quickly transport heavy loads from one place to another with the least sways possible and accurately position them at a target point to improve productivity and safety. Since the demand for automation of crane systems has increased, numerous control strategies for cranes have been increasingly developed [1]. Open-loop techniques such as input shaping approaches [2]–[5] are easy and cost-effective to implement without additional sensors. However, they are highly sensitive to unknown external disturbances (e.g., frictional forces), since the control input is predetermined and not adjusted during motion. Thus, various closed-loop techniques have been proposed: model predictive control [6], [7], energy-based control [8]–[10], intelligent control approaches [11], [12], sliding mode control [13]–[16], Lyapunov-based control [17],

nonlinear control methods [18]–[20], and other methods [21], [22]. In addition, adaptive fuzzy control was presented in [23] to address actuator dead zones. An observer-based nonlinear control method to avoid actuator saturation was proposed in [24]. Some authors proposed motion planning-based tracking control by exploiting the flatness property of cranes, which is useful to design trajectories and tracking controllers [25]–[30].

Feedback control has two objectives in the case of cranes: to follow a desired (non quasi-static) load trajectory, and to eliminate sway due to external disturbances and uncertain parameters. Both design and tracking of aggressive load trajectories require knowledge of the nonlinear model of the crane. In addition, for both tracking and sway elimination, knowledge (measurement or estimation) of the load position, sway angles, and frictional forces is necessary. Various feedback control techniques have been presented under the assumption that continuous measurements of the sway angles are available using sensors such as rotary encoders.

The associate editor coordinating the review of this manuscript and approving it for publication was Sun Junwei[ID].

Continuous measurements of sway angles are usually realized by a mechanism in contact with the cable, which is usually feasible only in laboratory environments. Such measurement systems are currently not applied to industrial crane systems to the best of our knowledge because they lack sufficient reliability and robustness and introduce extra wiring and additional potential failure causes. The direct measurements of the load position and frictional forces are also unreliable or nonexistent in real crane systems. In real applications, only motor positions are easily measured, so issues in the practical implementation of advanced feedback control techniques involve the availability of estimation techniques that provide robust estimates of unavailable signals needed by the control laws.

The estimation of sway angle is impeded by the unknown inputs (frictions) and dead zone. Many attempts to estimate the sway angle have been accomplished by employing different types of additional sensors, such as load cells [31], IMU sensors [32], [33], and vision sensors [34], [35], to overcome the unknown frictions and dead zones, despite increasing complexity for system integration. Meanwhile, various disturbance observers and similar techniques are designed to cancel the effect of frictions and dead zones on control inputs to improve the steady-state tracking results [36]–[39]. However, the performance of these disturbance observers may not be guaranteed, unless the sway angle is available or the cranes are initially in equilibrium.

In this work, an adaptive unscented Kalman filtering technique is developed to estimate both state variables and unknown inputs. Standard versions of the Kalman filter (KF), including nonlinear filters such as EKF and UKF, use constant noise/uncertainty covariance matrices Q and R, i.e., a priori knowledge about the noise properties. If the uncertainty covariance matrices are inconsistent with the real uncertainty between the system and the deterministic model in the KFs, such KFs will diverge or be biased. To solve this problem, standard KFs have been combined with various adaptation techniques. On-line estimation techniques and scaling techniques for noise covariance matrices result in a family of adaptive KFs [40]–[44].

The adaptation technique in this paper is technically a mix of estimation techniques and selective-scaling techniques for the process noise covariance matrix Q, and its concept is first suggested in [45]. Indeed, the estimation of Q is necessary in systems with unknown input disturbances, because the statistical property (covariance) of process noise usually changes over time. The derived estimation formula for Q is valid when the actual covariance of the process noise is assumed to slowly change. However, in practice, this assumption is not true for the crane system that experiences rapidly (step-like) changing disturbances such as friction. Thus, the selective scaling technique is required to tune the estimate of Q to prevent diverging and improve the convergence rate of the Kalman filter. Furthermore, we propose a condition-based use of the selective scaling method to deal with a transient estimation phase. When inaccurate transient estimates are

used for the feedback, the control mechanism results in an unexpected state transition from the filter viewpoint, which leads to excessive scaling of Q and prevents the filter from reaching a steady state. This problem can be resolved by the conditional usage of the selective scaling technique.

We exploit the flatness property (exact linearization) of the crane system to avoid any linearization approximations in the controller design process. The contribution of the paper is to implement the flatness-based control law using the proposed filter without being supported by any additional sensors. The proposed filtering technique is highlighted by the fact that the state variables and unknown input disturbances can be simultaneously estimated, considering the nonlinear model and a conditional selective scaling-based adaptive estimation technique. The simulation results show that the proposed filtering technique is suitable for the control of cranes.

The remainder of the paper is as follows. An overall structure of observer-based feedback linearization and input compensation for flatness-based motion control is presented in Section II. Section III describes an extension of the adaptive UKF algorithm to a continuous-discrete stochastic system and the detailed adaptation laws, including a condition-based selective scaling law. In addition, a variant of the adaptation law according to the discretization of the continuous-time nonlinear crane system is discussed in detail. A set of simulation results of estimation and tracking control is shown in Section IV. Section V concludes the paper with a summary.
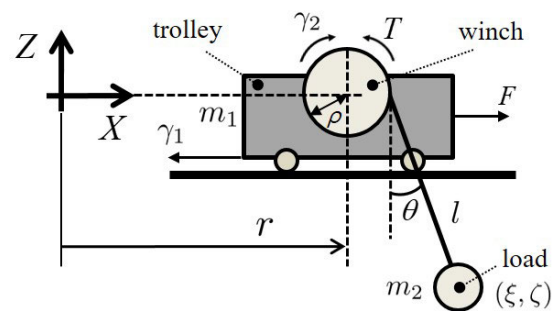
FIGURE 1. The two-dimensional overhead crane.

II. CONTROL SYNTHESIS
A. CRANE DYNAMICS AND FLATNESS PROPERTY
The dynamic equations of the 2D crane in Figure 1 can be derived using the Lagrangian method (e.g., [26], [29]) so that the generalized coordinates are selected as r, l, and θ: the trolley displacement, cable length, and sway angle of the suspended load w.r.t. the vertical, respectively. Then, the second order dynamics is obtained as

$$M \begin{bmatrix} \ddot{r} \\ \ddot{l} \\ \ddot{\theta} \end{bmatrix} + h = \begin{bmatrix} F \\ -\dfrac{T}{\rho} \\ 0 \end{bmatrix}, \tag{1}$$

$$M = \begin{bmatrix} m_1 + m_2 & m_2 \sin\theta & m_2 l \cos\theta \\ m_2 \sin\theta & m_2 + \dfrac{J}{\rho^2} & 0 \\ m_2 l \cos\theta & 0 & m_2 l^2 \end{bmatrix}, \tag{2}$$

$$h = \begin{bmatrix} -m_2\,l\dot{\theta}^2\sin\theta + 2\,m_2\dot{\theta}\dot{l}\cos\theta \\ -m_2\,l\dot{\theta}^2 - m_2 g\cos\theta \\ m_2\,l(2\dot{l}\dot{\theta} + g\sin\theta) \end{bmatrix}, \qquad (3)$$

where F and T are the driving forces applied for traveling and hoisting actions, m_1 and m_2 are masses of the trolley and load, J is the moment of inertia for the winch with a radius of ρ, and g is the gravitational acceleration. It is assumed that the cable that connects the load and the winch is mass-less and rigid, and the sway of load remains within $-\pi < \theta < \pi$. In this work, a trajectory tracking control approach using the flatness property of cranes is considered to achieve anti-sway positioning for underactuated loads. The flatness property is particularly advantageous for solving both trajectory planning and tracking control.

The flatness is a property of the system, which implies that a nonlinear system can be exactly transformed into a linear system using an output feedback scheme. A nonlinear system $\dot{x} = f(x, u)$ is differentially flat if one can find a set of variables, which is called flat output y, such that the state x and input u can be expressed in terms of y and a finite number of its time derivatives.

The crane system with $x = [r, l, \theta, \dot{r}, \dot{l}, \dot{\theta}]^T$ and $u = [F, T]^T$ is differentially flat [26]–[28]. The flat output can be chosen as

$$y = \begin{bmatrix} \xi \\ \zeta \end{bmatrix} = \begin{bmatrix} r + \rho + l\sin\theta \\ -l\cos\theta \end{bmatrix},$$

such that

$$x = \alpha(y, \dot{y}, \ddot{y}, y^{(3)}),$$
$$u = \beta(y, \dot{y}, \ddot{y}, y^{(3)}, y^{(4)}),$$

where ξ and ζ, which are components of y, are differentially independent as the Cartesian coordinates of load, which is obtained from geometric constraints.

B. FEEDBACK LINEARIZATION
The linearization scheme with dynamic feedback exploiting the flatness property is shown in Figure 2. Dynamic feedback is largely divided into static feedback and dynamic compensator. The dynamic compensator is designed as

$$\begin{bmatrix} F \\ T \end{bmatrix} = \Psi \begin{bmatrix} \mu_1 \\ \ddot{\theta} \end{bmatrix} + \psi, \qquad (4)$$

$$\Psi = \begin{bmatrix} m_2\sin\theta & -m_1 l\sec\theta \\ \dfrac{m_2\rho^2 + J}{\rho} & -\dfrac{J}{\rho}l\tan\theta \end{bmatrix}, \qquad (5)$$

$$\psi = \begin{bmatrix} -m_2 g\sin\theta\cos\theta - m_1\sec\theta(2\dot{l}\dot{\theta} + g\sin\theta) \\ m_2 g\rho\cos\theta - \dfrac{J}{\rho}l\dot{\theta}^2 - \dfrac{J}{\rho}\tan\theta(2\dot{l}\dot{\theta} + g\sin\theta) \end{bmatrix}, \qquad (6)$$

$$\dot{\mu} = \begin{bmatrix} \dot{\mu}_1 \\ \dot{\mu}_2 \end{bmatrix} = \begin{bmatrix} \mu_2 \\ \ddot{\eta} \end{bmatrix}, \qquad (7)$$

where $\mu_1(=\eta)$ and $\mu_2(=\dot{\eta})$ are additional states owned by the dynamic compensator, and η is the acceleration in the
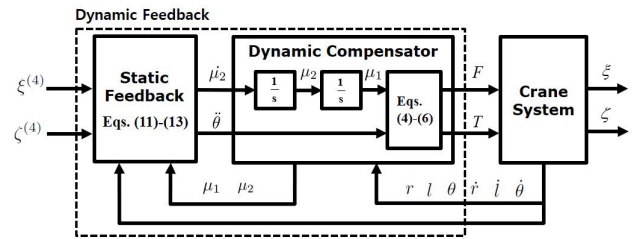
FIGURE 2. Feedback linearization scheme.

cable direction, which is defined by

$$\eta = -\frac{T_L}{m_2} + g\cos\theta = \ddot{r}\sin\theta + \ddot{l} - l\dot{\theta}^2$$

T_L is the tension exerted by the cable. By integrating the system (1)-(3) and dynamic compensator (4)-(7), one can obtain the extended model as follows:

$$\dot{\bar{x}} = \bar{f}(\bar{x}, \bar{u}) \qquad (8)$$

with

$$\bar{x} = [r, l, \theta, \dot{r}, \dot{l}, \dot{\theta}, \mu_1, \mu_2]^T, \qquad (9)$$
$$\bar{u} = [\dot{\mu}_2, \ddot{\theta}]^T. \qquad (10)$$

Then, the extended system (8)-(10) is combined with static feedback, whose equations are derived by taking the time derivative of y to order 4:

$$\begin{bmatrix} \dot{\mu}_2 \\ \ddot{\theta} \end{bmatrix} = \Phi\left(\begin{bmatrix} \xi^{(4)} \\ \zeta^{(4)} \end{bmatrix} - \phi\right), \qquad (11)$$

$$\Phi = \begin{bmatrix} \sin\theta & \mu_1\cos\theta - g\cos 2\theta \\ -\cos\theta & \mu_1\sin\theta - g\sin 2\theta) \end{bmatrix}^{-1}, \qquad (12)$$

$$\phi = \begin{bmatrix} 2\mu_2\dot{\theta}\cos\theta - \dot{\theta}^2(\mu_1\sin\theta - 2g\sin 2\theta) \\ 2\mu_2\dot{\theta}\sin\theta + \dot{\theta}^2(\mu_1\cos\theta - 2g\cos 2\theta) \end{bmatrix}. \qquad (13)$$

This yields the linear system described by

$$\dot{x}' = Ax' + Bu' \qquad (14)$$

with

$$x' = [\xi, \dot{\xi}, \ddot{\xi}, \xi^{(3)}, \zeta, \dot{\zeta}, \ddot{\zeta}, \zeta^{(3)}]^T, \qquad (15)$$
$$u' = [\xi^{(4)}, \zeta^{(4)}], \qquad (16)$$

where x' is the new state vector whose components are the flat output and its time derivatives, which govern the transition of the linear system (14). The dynamic feedback renders a decoupled linear input-output map from the new input u' to the flat output y. The missing new state variables are represented in terms of x and μ as follows:

$$\dot{\xi} = \dot{r} + \dot{l}\sin\theta + l\dot{\theta}\cos\theta,$$
$$\ddot{\xi} = \mu_1\sin\theta - g\sin\theta\cos\theta,$$
$$\xi^{(3)} = \mu_2\sin\theta + \mu_1\dot{\theta}\cos\theta - g\dot{\theta}\cos 2\theta,$$
$$\dot{\zeta} = -\dot{l}\cos\theta + l\dot{\theta}\sin\theta,$$
$$\ddot{\zeta} = -\mu_1\cos\theta - g\sin^2\theta,$$
$$\zeta^{(3)} = -\mu_2\cos\theta + \mu_1\dot{\theta}\sin\theta - g\dot{\theta}\sin 2\theta.$$

C. DESIGN OF THE TRACKING CONTROLLER

We suppose that the reference load trajectories $(\xi_r(t), \zeta_r(t))$ are sufficiently smooth to have their time derivatives up to order 4. For the resulting system defined by (14)-(16), one can easily design a tracking controller based on the following linear feedback law:

$$u'_1 = \xi_r^{(4)} + k_{\xi,3} e_\xi^{(3)} + k_{\xi,2} \ddot{e}_\xi + k_{\xi,1} \dot{e}_\xi + k_{\xi,0} e_\xi, \quad (17)$$

$$u'_2 = \zeta_r^{(4)} + k_{\zeta,3} e_\zeta^{(3)} + k_{\zeta,2} \ddot{e}_\zeta + k_{\zeta,1} \dot{e}_\zeta + k_{\zeta,0} e_\zeta, \quad (18)$$

where e_ξ and e_ζ are the tracking errors defined by

$$e_\xi = \xi_r - \xi,$$
$$e_\zeta = \zeta_r - \zeta.$$

By substituting $u'_1 = \xi^{(4)}$ and $u'_2 = \zeta^{(4)}$ into (17) and (18), we can obtain error dynamics of the closed-loop system as follows:

$$e_\xi^{(4)} + k_{\xi,3} e_\xi^{(3)} + k_{\xi,2} \ddot{e}_\xi + k_{\xi,1} \dot{e}_\xi + k_{\xi,0} e_\xi = 0, \quad (19)$$

$$e_\zeta^{(4)} + k_{\zeta,3} e_\zeta^{(3)} + k_{\zeta,2} \ddot{e}_\zeta + k_{\zeta,1} \dot{e}_\zeta + k_{\zeta,0} e_\zeta = 0. \quad (20)$$

If the error dynamics (19) and (20) are made stable by an appropriate choice of the control gains $k_{\xi,i}$ and $k_{\zeta,i}$ for $i = 0, \ldots, 3$, the tracking errors exponentially converge to zeros. The control gains can be simply determined using the pole placement method. Considering four-fold poles as desired ones, the characteristic polynomials of the closed-loop error dynamics are such that

$$(s - a_\xi)^4 = s^4 - k_{\xi,3} s^3 + k_{\xi,2} s^2 - k_{\xi,1} s + k_{\xi,0},$$
$$(s - a_\zeta)^4 = s^4 - k_{\zeta,3} s^3 + k_{\zeta,2} s^2 - k_{\zeta,1} s + k_{\zeta,0},$$

Thus, the control gains are determined by

$$k_{\xi,3} = 4a_\xi, \quad k_{\xi,2} = 6a_\xi^2, \; k_{\xi,1} = 4a_\xi^3, \; k_{\xi,0} = a_\xi^4, \quad (21)$$

$$k_{\zeta,3} = 4a_\zeta, \quad k_{\zeta,2} = 6a_\zeta^2, \; k_{\zeta,1} = 4a_\zeta^3, \; k_{\zeta,0} = 4a_\zeta^4, \quad (22)$$

where $a_\xi < 0$ and $a_\zeta < 0$ are the desired, four-fold poles.

D. MOTION PLANNING

For a rest-to-rest motion planning of the load, it is necessary for the reference trajectories to satisfy the following initial and final conditions:

$$\xi_r(t_I) = \xi_I, \quad \dot{\xi}_r(t_I) = \ddot{\xi}_r(t_I) = \xi_r^{(3)}(t_I) = \xi_r^{(4)}(t_I) = 0, \quad (23)$$

$$\xi_r(t_F) = \xi_F, \quad \dot{\xi}_r(t_F) = \ddot{\xi}_r(t_F) = \xi_r^{(3)}(t_F) = \xi_r^{(4)}(t_F) = 0, \quad (24)$$

$$\zeta_r(t_I) = \zeta_I, \quad \dot{\zeta}_r(t_I) = \ddot{\zeta}_r(t_I) = \zeta_r^{(3)}(t_I) = \zeta_r^{(4)}(t_I) = 0, \quad (25)$$

$$\zeta_r(t_F) = \zeta_F, \quad \dot{\zeta}_r(t_F) = \ddot{\zeta}_r(t_F) = \zeta_r^{(3)}(t_F) = \zeta_r^{(4)}(t_F) = 0, \quad (26)$$

where (ξ_I, ζ_I) is the set point of the initial position at $t = t_I$, and (ξ_F, ζ_F) is that of the final position at $t = t_F > t_I$.

It is reasonable to select a set of polynomials to provide smooth and continuous motion with some level of continuous

derivatives [55]. With the polynomial interpolation method using the given conditions (23) and (24), the reference load trajectory $\xi_r(t)$ for the X-axis can be generated as follows:

$$\xi_r(t) = \xi_I + (\xi_F - \xi_I) \sum_{i=5}^{9} c_i \left(\frac{t - t_I}{t_F - t_I} \right)^i, \quad t \in [t_I, t_F],$$

with $c_5 = 126$, $c_6 = -420$, $c_7 = 540$, $c_8 = -315$, and $c_9 = 70$. If $\xi_r(t) \neq \xi_I$, the desired path of the load in the XZ-plane can be designed by considering the following geometric relation: $\zeta_r(t) = \zeta_r(\xi_r(t))$ [46]. In this work, a parabolic path is considered so that reference trajectory $\zeta_r(t)$, which satisfies conditions (25) and (26), is generated as follows:

$$\zeta_r(t) = \zeta_r(\xi_r(t)) = a(\xi_r(t) - \xi_m)^2 + \zeta_m,$$
$$a = \frac{\zeta_I - \zeta_m}{(\xi_I - \xi_m)^2},$$
$$\xi_m = \frac{\sqrt{\frac{\zeta_I - \zeta_m}{\zeta_F - \zeta_m}} \xi_F + \xi_I}{\sqrt{\frac{\zeta_I - \zeta_m}{\zeta_F - \zeta_m}} + 1},$$

where ζ_m is a design parameter that determines a and ξ_m.

E. OBSERVER-BASED CONTROL AND INPUT COMPENSATION

The control scheme described above requires that all state variables are available for feedback and there be no disturbances. However, in practical crane applications, only displacements r and l are usually measured, and the crane system is disturbed by unknown inputs such as friction and traction. Considering the disturbance inputs that act on the trolley and winch, we can rewrite the state-space model of the crane system as

$$\dot{x} = f(x, \tilde{u}),$$

with $\tilde{u}$, the disturbed input vector specified by

$$\tilde{u} = \begin{bmatrix} F - \gamma_1 \\ T + \gamma_2 \end{bmatrix} = u + \Lambda u_d, \quad (27)$$

where $u_d = [\gamma_1, \gamma_2]^T$ is the additive disturbance input vector.

An alternative is to develop an observer that can simultaneously estimate the state variables and unknown inputs so that the state feedback and disturbance rejection can be collaboratively achieved. The observer-based control strategy is illustrated in Figure 3. The input to the crane system and observer is replaced with the compensated input u_c:

$$u_c = u - \Lambda \hat{u}_d,$$

where $\hat{u}_d$ is the estimate of the disturbance input.

The simultaneous estimation problem for a crane system with unknown input disturbances is extremely challenging due to the nonlinearity and inconsistent information about the model and process uncertainties. To tackle these difficulties, we propose an adaptive unscented Kalman filter with a condition-based selective scaling (AUKF-CSS) technique
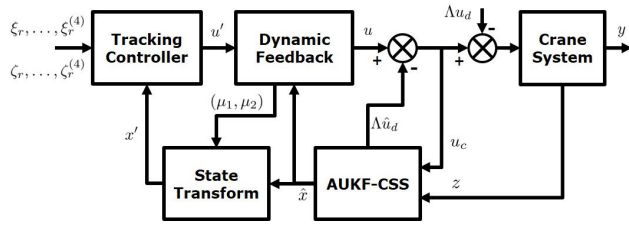
FIGURE 3. Architecture of the proposed AUKF based crane control.

that can handle nonlinear equations and adapt to the process uncertainty worsened by unmodeled disturbance inputs. A specific algorithm of the proposed AUKF-CSS is shown in Section III.

III. ADAPTIVE UNSCENTED KALMAN FILTER

In this section, a novel adaptive UKF is discussed in detail to solve the simultaneous state and unknown input estimation problem, which ranges from constructing an extended state-space model including the unknown inputs as state variables, through discretizing, to adapting to inconsistent process uncertainty.

A. MODEL DESCRIPTION FOR KALMAN FILTERING

Consider a continuous-discrete stochastic system:

$$dx(t) = f(x(t), \tilde{u}(t))dt + dw(t), \qquad (28)$$
$$z(k) = H_1 x(t_k) + v(k),$$

where $x(t) \in \mathbb{R}^n$ is the state vector, $\tilde{u}(t) \in \mathbb{R}^m$ is the disturbed input vector, and $z(k) \in \mathbb{R}^p$ is the measurement vector taken at $t = t_k$ via a digital processor. In addition, $w(t)$ is Brownian motion with diagonal diffusion matrix $Q_1(t)$, and $v(k)$ is zero-mean Gaussian measurement noise with covariance matrix $R(k)$. Here, it is assumed that the disturbance is additive to the known input such that $\tilde{u}(t) = u(t) + \Lambda u_d(t)$, where $u_d(t) \in \mathbb{R}^q$ for $q \leq p$ is the disturbance input vector, and Λ is a known constant matrix. We suppose that the measurement equation is linear. This holds true for many applications, including mechanical systems, where measurements are obtained on configuration variables and their derivatives, or the linear dependence of measurements on the state variables can be ensured by nonlinear coordinate transformation [47]–[49].

We encounter the problem of continuous-discrete unscented Kalman filtering (CD-UKF) (see [50], [51] for a detailed discussion on the CD-UKF). A possibility is to use the Euler method to derive a numerical solution of the stochastic differential equation (28) for the time increment, $\Delta t = t_{k+1} - t_k$. Then, one can obtain

$$x(t_{k+1}) = x(t_k) + f(x(t_k), \tilde{u}(t_k))\Delta t + \Delta w(t_k) + o(\Delta t^2),$$

where $\Delta w(t_k) \sim \mathcal{N}(0, Q_1(t_k)\Delta t)$. $o(\Delta t^2)$ is higher-order terms with powers of Δt greater than or equal to 2, and the higher-order terms can be ignored when Δt is sufficiently close to zero.

Assuming that the behavior of the disturbance inputs is also a Brownian motion with diagonal diffusion matrix $Q_2(t)$, we model the stochastic process of $u_d(t_k)$ for the time increment as the random walk process:

$$u_d(t_{k+1}) = u_d(t_k) + \Delta w_d(t_k), \qquad (29)$$

where $\Delta w_d(t_k) \sim \mathcal{N}(0, Q_2(t_k)\Delta t)$. Similar to the joint parameter-state estimation approach suggested in [52], [53], the extended model with the augmented state vector,

$$x_a(t_k) = [x(t_k), u_d(t_k)]^T,$$

is introduced as follows:

$$x_a(t_{k+1}) = \begin{bmatrix} x(t_k) + f(x(t_k), \tilde{u}(t_k))\Delta t \\ u_d(t_k) \end{bmatrix} + \begin{bmatrix} \Delta w(t_k) \\ \Delta w_d(t_k) \end{bmatrix},$$
$$x_a(t_{k+1}) = f_a(x_a(t_k), u(t_k)) + \Delta w_a(t_k), \qquad (30)$$
$$z(k) = \begin{bmatrix} H_1 & 0 \end{bmatrix} x_a(t_k) + v(k) = H x_a(t_k) + v(k), \quad (31)$$

where $\Delta w_a(t_k) \sim \mathcal{N}(0, Q(t_k)\Delta t)$ such that $Q(t_k) = \text{diag}\{Q_1(t_k), Q_2(t_k)\}$.

Provided that the extended model defined by (30) and (31) is observable, a discrete-time UKF can be constructed. With the zero-order holding assumption that the variables are piecewise constant over the sampling interval, we will write $x_a(k) := x_a(t_k), u(k) := u(t_k)$, and $\Delta w_a(k) := \Delta w_a(t_k)$ where $\Delta w_a(k) \sim \mathcal{N}(0, Q(k))$ so that $Q(k) := Q(t_k)\Delta t$.

B. ADAPTIVE UKF ALGORITHM

In the simultaneous estimation problem, the measurement noise covariance $R(k)$ is assumed to be completely known independent of k with reasonable accuracy; hence, $R(k) = R$. However, the process noise covariance matrix $Q(k)$ is considered time-varying, so an adaptation technique is required for its estimation.

As usual, we distinguish the estimates of the time update (prediction) phase and the measurement update phase. For step k, we denote by $\hat{x}_a^-(k)$ (resp. $P^-(k)$) the state estimation (resp. its covariance matrix) after the prediction phase and by $\hat{x}_a(k)$ (resp. $P(k)$) after the measurement update. The unscented transform [54] of estimate $\hat{x}_a(k-1)$ and that of covariance matrix $P(k-1)$ under nonlinear mapping f_a with fixed $u(k-1)$ are denoted by $UT\{f(\cdot, u(k-1)), \hat{x}_a(k-1), P(k-1)\}$ so that the time update phase of the AUKF (through $\hat{Q}$: the adaptation of Q) reads

$$[\hat{x}_a^-(k), \bar{P}(k)] = UT\{f_a(\cdot, u(k-1)), \hat{x}_d(k-1), P(k-1)\},$$
$$P^-(k) = \bar{P}(k) + \hat{Q}(k-1).$$

Since the measurement equation (31) is linear, the time update phase is combined with a linear measurement update phase, which is represented by

$$\hat{z}^-(k) = H\hat{x}_a^-(k),$$
$$P_{zz}(k) = HP^-(k)H^T + R(k),$$
$$K(k) = P^-(k)H^T P_{zz}^{-1}(k),$$
$$\hat{x}_a(k) = \hat{x}_a^-(k) + K(k)(z(k) - \hat{z}^-(k)),$$
$$P(k) = P^-(k) - K(k)P_{zz}(k)K^T(k),$$

where $K(k)$ and $P_{zz}(k)$ are the Kalman gain and innovation matrix, respectively.

The AUKF further includes the adaptation phase that provides $\hat{Q}(k)$ to be used for step $k+1$ in the following form:

$$\hat{Q}(k) = S(k)\hat{Q}^-(k),$$

where $\hat{Q}^-(k)$ is an estimated process noise covariance matrix, and $S(k)$ is a so-called scaling matrix.

C. ADAPTATION PHASE

1) ESTIMATION OF Q

Let $\Delta w_a(k) = \sqrt{\Delta t}\omega(k)$, where $\omega(k) \sim \mathcal{N}(0, \frac{Q(k)}{\Delta t})$ is the Gaussian noise sequence, which is discussed in a discrete-time adaptation scheme. We apply the innovation-based adaptation method [44] derived from the maximum likelihood (ML) cost function using a window of N samples:

$$\sum_{j=j_0}^{k} \frac{Q(j)}{\Delta t} = \sum_{j=j_0}^{k} \Delta\hat{x}_a(j)\Delta\hat{x}_a(j)^T + \sum_{j=j_0}^{k} (P(j) - \bar{P}(j)) \quad (32)$$

where $\Delta\hat{x}_a(j) = K(j)\tilde{z}(j)$ is the state correction sequence, and $\tilde{z}(j) = z(j) - \hat{z}^-(j)$ is the innovation. For a window of N samples $j_0 = k - N + 1$.

With the assumption that $Q(k)$ is slowly changing inside the observation window of length N, let us define the estimate $\hat{Q}^-(k)$ as

$$\hat{Q}^-(k) := \frac{1}{N} \sum_{j=j_0}^{k} Q(j). \quad (33)$$

Substituting (33) into (32) yields

$$\hat{Q}^-(k) = \frac{\Delta t}{N} \sum_{j=j_0}^{k} (\Delta\hat{x}_a(j)\Delta\hat{x}_a^T(j) + P(j) - \bar{P}(j)).$$

Recall that the process noise is supposed to be white Gaussian noise, whose components are considered a sequence of serially uncorrelated random variables so that off-diagonal elements are not up for discussion. Therefore,

$$\hat{Q}_{ii}^-(k) = \frac{\Delta t}{N} \sum_{j=j_0}^{k} \left(\Delta\hat{x}_{a,i}^2(j) + P_{ii}(j) - \bar{P}_{ii}(j) \right), \quad (34)$$

where $i = 1, \ldots, n+q$. The terms $\bar{P}_{ii}(j)$ may make the expression on the right-hand side negative. Some authors eliminate this problem using a steady-state assumption, i.e., $P_{ii}(j) \cong \bar{P}_{ii}(j)$; then equation (34) becomes

$$\hat{Q}_{ii}^-(k) = \frac{\Delta t}{N} \sum_{j=j_0}^{k} \Delta\hat{x}_{a,i}^2(j), \quad \text{for } k \geq 1 \quad (35)$$

with initial values for $j \leq 0$

$$\Delta\hat{x}_{a,i}(1-N) = \cdots = \Delta\hat{x}_{a,i}(-1) = \Delta\hat{x}_{a,i}(0) = 0.$$

The estimates of Q in (35) are subject to the sampling interval in contrast to the original adaptation formula derived for the discrete-time system in [44]. The sampling interval is an important factor that determines the convergence of the adaptive Kalman filter that utilizes the discretized model of a continuous-time system, which should not be overlooked in practical algorithm implementation.

2) CONDITION-BASED SELECTIVE SCALING LAW

If disturbance input u_d changes in a different manner from the stochastic process (random walk movement) defined by (29), the estimated matrix $\hat{Q}^-(k)$ is not entirely reliable. Definitely, in such situations, the filter with the extended model experiences considerable process uncertainty due to the lack of a deterministic dynamic model for the disturbance input. Therefore, it is necessary to appropriately increase $\hat{Q}^-(k)$ to ensure a quicker convergence of the filter, which can be achieved using a scaling technique.

Without loss of generality, measurement matrix H can have an identity matrix component of size p, if necessary, by performing the state transformation and/or rearrangement of state variables. When the measurement matrix is given by $H = [I_p \ 0]$, diagonal matrix $\hat{Q}^-(k)$ can be decomposed into $\hat{Q}^-(k) = \text{diag}\{\hat{Q}_{1,m}^-(k), \hat{Q}_{1,\bar{m}}^-(k), \hat{Q}_2^-(k)\}$, where $\hat{Q}_{1,m}^-(k)$ and $\hat{Q}_{1,\bar{m}}^-(k)$ are the process uncertainties of the measured and unmeasured system states, respectively. Since the submatrix $\hat{Q}_{1,m}^-(k)$ is reliably corrected using the measurements, it is not our concern. Only the other submatrices $\hat{Q}_{1,\bar{m}}^-(k)$ and $\hat{Q}_2^-(k)$ are selectively tuned by scaling factors.

The (selective) scaling of Q tends to increase *a posteriori* error covariance matrix $P(k)$ [45]. This property is important for a quick convergence property of the filter, but, it implies that the filter is in a transient phase, since the estimates may not be sufficiently accurate in the mean squared error sense. In closed-loop systems where the estimates are directly used for control purposes, the control mechanism, including input compensation, can result in the indiscriminate scaling of Q, which prevents the filter from reaching a steady-state. This phenomenon can be seriously observed when there are initial errors between the actual outputs and the desired outputs. If one can introduce conditions to timely apply the scaling technique, the control and estimation performance can be greatly improved.

First, we suppose that $\Delta\hat{x}_a(k)$ is a Gaussian random vector with

$$\text{E}[\Delta\hat{x}_a(k)] = 0 \quad (36)$$
$$\text{Cov}(\Delta\hat{x}_a(k), \Delta\hat{x}_a(k)) = G(k).$$

Using the relations $\Delta\hat{x}_a(k) = K(k)\tilde{z}(k)$ and $P_{zz}(k) := E[\tilde{z}(k)\tilde{z}^T(k)]$ and the steady-state assumption that yields a constant Kalman gain, the covariance $G(k)$ can be approximated as a function of the filter-computed matrices:

$$\tilde{G}(k) = K(k)P_{zz}(k)K^T(k). \quad (37)$$

Now, it is possible to introduce the statistical evaluation index that arises from the Gaussian random variables

normalized using (36) and (37):

$$\lambda_i(k) = \frac{\Delta \hat{x}_{a,i}^2(k)}{\tilde{G}_{ii}(k)} \sim \chi_1^2, \quad i = 1, \dots, n+q,$$

where $\lambda_i(k)$ has the Chi-squared distribution with 1 degree of freedom. The chi-square statistic $\lambda_i(k)$, which is obtained at step $k \geq 1$, is used as a measure to detect anomalies caused by changes in unknown inputs. When a condition is given for $\lambda_i(k)$, the filter can determine whether to enable the scaling of $\hat{Q}_{ii}^-(k)$ at step $k+1$. The detailed law of the condition-based selective scaling is described as follows:

- For $i = 1, \dots, p$, $S_{ii}(k)$ is always 1 without regard to $\lambda_i(k)$:

$$S_{ii}(k) = 1, \quad \forall \lambda_i(k),$$

- For $i = p+1, \dots, n$, $S_{ii}(k)$ is conditionally 1 or a value greater than 1, the ratio of an estimated variance to the filter-computed variance for the state correction sequence:

$$S_{ii}(k) = \begin{cases} 1, & \lambda_i(k) < \bar{\lambda}_i \\ \max\left(1, \dfrac{\hat{G}_{ii}(k)}{\tilde{G}_{ii}(k)}\right), & \lambda_i(k) \geq \bar{\lambda}_i \end{cases}$$

- For $i = n+1, \dots, n+q$, $S_{ii}(k)$ is conditionally 1 or the value greater than 1 that initializes $\hat{Q}_{ii}(k)$:

$$S_{ii}(k) = \begin{cases} 1, & \lambda_i(k) < \bar{\lambda}_i \\ \max\left(1, \dfrac{\hat{Q}_{ii}(0)}{\hat{Q}_{ii}^-(k)}\right), & \lambda_i(k) \geq \bar{\lambda}_i \end{cases}$$

where $\bar{\lambda}_i$ is an upper-tail critical value for the chi-square distribution of $\lambda_i(k)$ to detect anomalies, and $\hat{G}(k)$ is the statistically estimated covariance matrix of the state correction sequence using N windowed samples. With the additional assumption that the elements of $\Delta \hat{x}_a(k)$ are uncorrelated, $\hat{G}(k)$ can be simply obtained as:

$$\hat{G}(k) = \frac{\hat{Q}^-(k)}{\Delta t}.$$

The recursive algorithm of the AUKF-CSS is summarized in Figure 4.

IV. SIMULATION

In this section, the performance of the motion planning-based anti-sway control using the proposed AUKF-CSS is verified through extensive computer simulations.

A. SIMULATION SETUP

The crane parameters in the simulations are $m_1 = 4.552$ kg, $m_2 = 0.048$ kg, $g = 9.81$ m/s^2, $J = 3.802 \cdot 10^{-4}$ kg $\cdot$ m^2, and $\rho = 0.018$ m. The initial conditions of the control system are given by $x(0) = [0, 1.2, \theta(0), 0, 0, 0]^T$ and $\mu(0) = [0, 0]^T$. For tracking control, the desired four-fold poles of the
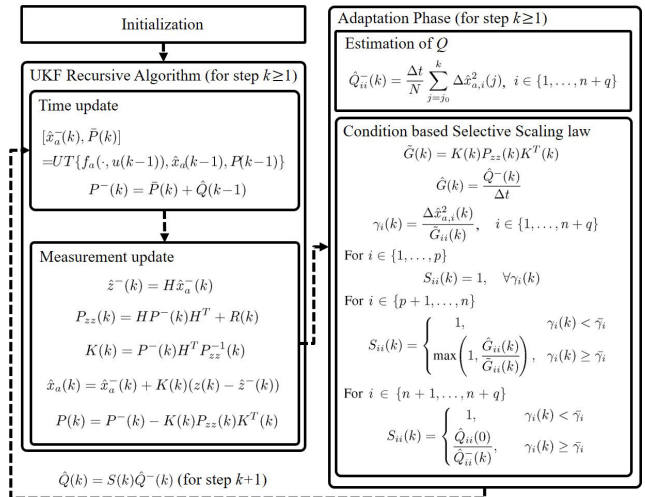
FIGURE 4. Recursive algorithm of the AUKF-CSS.

closed-loop dynamics (19) and (20) are set to $a_\xi = a_\zeta = -2$, so that the control gains are determined by (21) and (22).

The unknown disturbance input γ_i for $i = 1, 2$ in (27) is considered as Stribeck friction model, which is a function of the relative velocity $v_{r,i}$:

$$\gamma_i(v_{r,i}) = \sqrt{2e}(\Gamma_{brk,i} - \Gamma_{c,i}) e^{-\left(\frac{v_{r,i}}{v_{s,i}}\right)^2} \frac{v_{r,i}}{v_{s,i}}$$
$$+ \Gamma_{c,i} \tanh\left(\frac{v_{r,i}}{v_{c,i}}\right) + f_{v,i} v_{r,i}$$

where $v_{r,i}$ corresponds to $\dot{r}$ for $i = 1$ and $\dot{l}$ for $i = 2$, $\Gamma_{c,i}$ is the Coulomb friction force, $\Gamma_{brk,i}$ is the breakaway friction force, $v_{s,i}$ is the stribeck velocity threshold, $v_{c,i}$ is the Coulomb velocity threshold, and f_i is the viscous friction coefficient. Both $v_{s,i}$ and $v_{c,i}$ can be represented in terms of the breakaway friction velocity $v_{brk,i}$ as follows: $v_{s,i} = \sqrt{2} \cdot v_{brk,i}$ and $v_{c,i} = v_{brk,i}/10$. Specific values of the parameters for the friction models are given by $\Gamma_{c,1} = 0.1$, $\Gamma_{c,2} = 0.001$, $\Gamma_{brk,1} = 0.15$, $\Gamma_{brk,2} = 0.0015$, $v_{brk,1} = 0.0001$, $v_{brk,2} = 0.1$, $f_{v,1} = 0.01$, and $f_{v,2} = 0.0001$.

The AUKF-CSS is based on the unscented transform computed using a symmetric set of sigma points [52]. The augmented state vector and measurement vector for the AUKF-CSS are defined as $x_a = [r, l, \theta, \dot{r}, \dot{l}, \dot{\theta}, \gamma_1, \gamma_2]^T$ and $z = [r, l]^T$. The state transition models for γ_1 and γ_2 in the filter are assumed to be random walk processes (29). The measurement noise covariance matrix is held constant at all estimation steps. However, the process noise covariance matrix is the filter's self-adapting matrix, and its initial values are roughly chosen, except $\hat{Q}_2(0)$ must be carefully determined through empirical tests. For the condition-based selective scaling law, the upper-tail critical values are set to $\bar{\lambda}_3 = \bar{\lambda}_4 = \bar{\lambda}_5 = \bar{\lambda}_6 = 6.635$ (corresponding to a p-value of 0.01) and $\bar{\lambda}_7 = \bar{\lambda}_8 = 21.26$ (corresponding to a p-value of 4×10^{-6}). Although this value for $\bar{\lambda}_7$ and $\bar{\lambda}_8$ is quite large, it is required to avoid frequent initializations of $\hat{Q}_2(k)$.

TABLE 1. Initial setup for UKFs.

Symbol	Value	Remark
$\hat{x}(0)$	$[0\ 1.2\ 0\ 0\ 0\ 0\ 0\ 0]^T$	
$P(0)$	$\mathrm{diag}\{1.2\cdot 10^{-9}, 6.6\cdot 10^{-8}, 10^{-10}, 5\cdot 10^{-9}, 5\cdot 10^{-5}, 5\cdot 10^{-5}, 2\cdot 10^{-6}, 10^{-8}\}$	All
$R(k)$	$10^{-10}I_2$	filters
Δt	1 ms	
$Q(k)$	$\mathrm{diag}\{5\cdot 10^{-9}, 10^{-8}, 10^{-9}, 2\cdot 10^{-8}, 10^{-5}, 10^{-4}, 10^{-1}, 10^{-7}\}$	UKF
$\hat{Q}(0)$	$\mathrm{diag}\{5\cdot 10^{-9}, 10^{-8}, 10^{-9}, 2\cdot 10^{-8}, 10^{-5}, 10^{-4}, 10^{-1}, 10^{-7}\}$	Adapt.
$S(0)$	I_8	ver.
N	10	

From a control viewpoint, the performance of AUKF-CSS is compared with that of several filters: the conventional UKF and the AUKF-SS [45] of unconditionally applying a selective scaling technique. Configuration variables and their initial values of the considered UKFs are identical except for additional variables in the adaptation phase. Further information on the initial setup for different UKFs is summarized in Table 1.
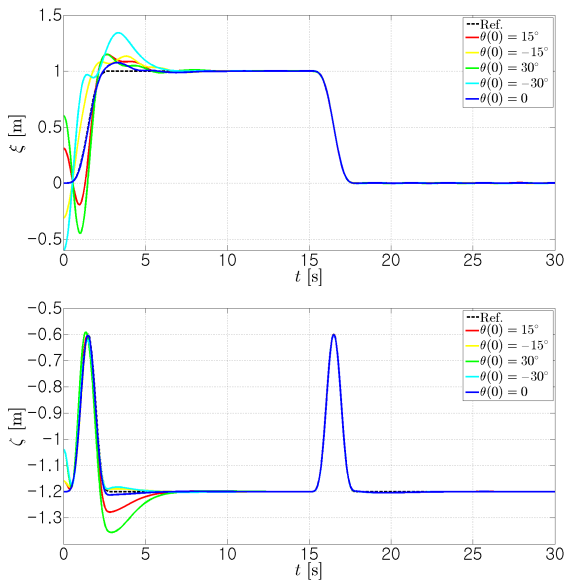
FIGURE 5. Tracking results in ξ and ζ for different initial angles of the load.

We consider the scenario where the load is transported along parabolic paths with the travel time of $t_F - t_I$. Two parabolic paths are planned: one is planned at $t = 0$ to examine the effect of the initial angle $\theta(0)$ on the estimation and control, and the other is planned at $t = 15$ to verify the convergence property of the steady-state AUKF-CSS.

B. SIMULATION RESULTS

The tracking results in coordinates ξ and ζ for different values of the initial angle of the load are shown in Figure 5. Despite the unknown frictions, the initial errors are successfully reduced over time. Overshoots occur oven in the case of $\theta(0) = 0$, which involves no initial position errors in ξ

and ζ, mainly because the AUKF-CSS with incomplete initial statistical knowledge is in a transient estimation phase. For all presented initial angles of the load, as expected, the second transport is satisfactorily achieved, so we can infer that the estimates of the AUKF-CSS converge to the actual values of the state variables and frictional inputs.

Figure 6 shows the estimation errors for θ and $\dot{\theta}$. Indeed, the AUKF-CSS can overcome the considerable process uncertainties caused by the unknown frictional inputs and reach a steady state, where the oscillating estimation errors of angular position are maintained within acceptable bounds. The steady-state filter estimates the actual angular position and its derivative properly without involving excessive errors in the second transport, unlike the first transport, especially for the case of $\theta(0) = 0$, since the filter has sufficiently accurate knowledge of $P(k)$ with respect to the captured state variables.
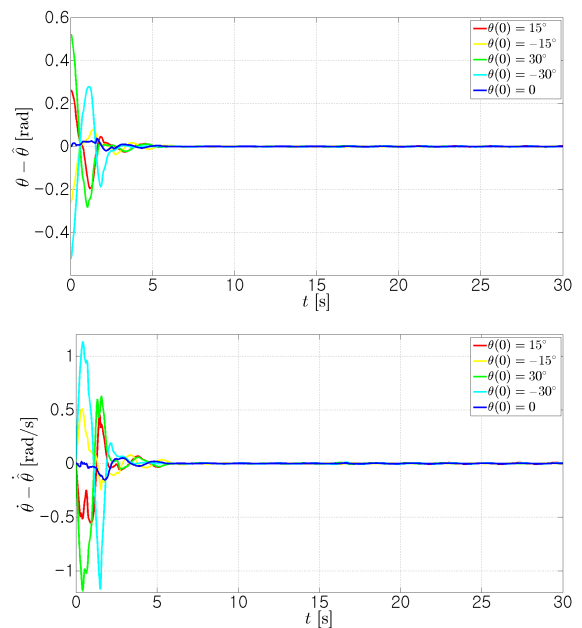
FIGURE 6. Estimation results of θ and $\dot{\theta}$ for different initial angles of the load.

Even if all crane state variables are exactly known and consequently available for feedback, and the crane system is initially in equilibrium, the influences of friction generally cause unwanted steady-state errors in the motion control. Figure 7 shows that the AUKF-CSS based control method, which can compensate the control inputs with the estimates regarding the frictional forces, considerably reduces the steady-state errors. The estimates of γ_1 and γ_2 are shown in Figure 8. Figure 9 presents the AUKF-CSS-based tracking results in the XZ-plane.

The superiority of the AUKF-CSS-based motion control is more clearly demonstrated compared to the motion controls using the UKF and AUKF-SS. Figure 10 illustrates the angular position of the load due to the motion control for the three UKFs. For the case of $\theta(0) = 0$, as shown in Figure 10(a),

FIGURE 7. Effectiveness of the input compensation using the AUKF-CSS.

FIGURE 8. Estimates of frictions γ_1 and γ_2.

FIGURE 9. AUKF-CSS based control results in X-Z plane.

the conventional UKF using $Q(k)$ as constant matrix, which is vulnerable to changes in the process noise caused by the

(a) $\theta(0) - \hat{\theta}(0) = 0°$

(b) $\theta(0) - \hat{\theta}(0) = 1°$

FIGURE 10. Angular positions under control using different UKFs.

FIGURE 11. Calculated control inputs and actual inputs under saturation and deadzone.

unknown frictional forces, results in a poor tracking performance; accordingly, the load sway cannot be suppressed. In contrast, when the adaptive versions of the UKF designed to adapt to the time-varying process noise are used for motion control, we observe that the load can be stabilized at the final position. However, Figure 10(b) shows that the AUKF-SS and the UKF are unreliable when there is initial error, although the initial error is quite small. Consequently, only the AUKF-CSS

(a) for travel time of 3s

(b) for travel time of 4.5s

FIGURE 12. Control results in the X-Z plane under saturation and deadzone.

(a) for travel time of 3s

(b) for travel time of 4.5s
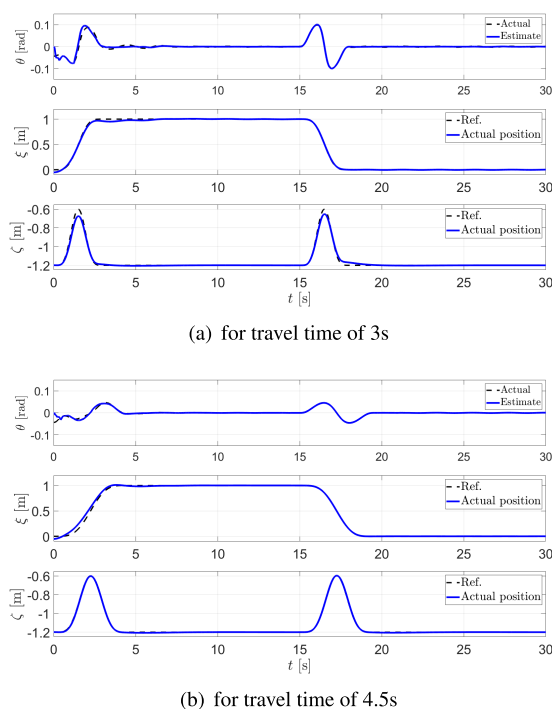
FIGURE 13. Estimation and tracking results under saturation and deadzone.

can achieve reliable estimation due to the condition-based timely use of the selective scaling of Q and enables anti-sway control, so that the load can be precisely positioned.

Further simulations are performed to demonstrate the effectiveness of the proposed filter-based flatness control

with a crane system having input saturation and deadzone. In the simulations, the control inputs are set to be limited by input boundary values such as input saturations, and the dead zones along with frictions are considered unknown inputs. The initial angular position of the load is $\theta(0) = -2.5°$. The calculated control inputs and actual inputs are illustrated in Figure 11, where the torque T required in equilibrium to hold the load is $T = mg\rho$. The input saturations may degrade the path-following performance independent of the performance of the filter, which is obviously observed for the second transport in Figure 12(a). However, as shown in Figure 12(b), considering the less aggressive trajectories can alleviate the input saturation problems, although at a loss in time efficiency. Figure 13 shows that the estimation and tracking errors in the steady state almost vanish due to the compensation mechanism for friction and deadzone.

V. CONCLUSION

In this paper, an observer-based motion control scheme is proposed for an underactuated overhead crane system to achieve anti-sway and precise positioning of the load. The fundamental control strategy considered is based on the flatness property of the crane. To develop the flatness-based motion control scheme for a crane system with unknown input disturbances, a reliable observer that can simultaneously estimate the state and disturbance is proposed for state feedback and disturbance rejection. Specifically, an adaptive unscented Kalman filter with a condition-based selective scaling technique (AUKF-CSS) is suggested to solve the simultaneous estimation problem under the control mechanism. The AUKF-CSS additionally includes the adaptation phase to adapt itself to considerable modeling (process) uncertainties caused by unknown disturbance. In the adaptation phase, first, the time-varying process noise covariance is estimated; second, to improve the convergence performance of the filter, the estimated process noise covariance matrix is tuned by the scale matrix, which is calculated according to the condition-based selective scaling law. Simulation results are provided to demonstrate that the proposed approach can achieve excellent motion control for different initial angles of load with no additional sensors even in the presence of unknown inputs.

REFERENCES

[1] L. Ramli, Z. Mohamed, A. M. Abdullahi, H. I. Jaafar, and I. M. Lazim, "Control strategies for crane systems: A comprehensive review," *Mech. Syst. Signal Process.*, vol. 95, pp. 1–23, Oct. 2017.

[2] Z. N. Masoud and M. F. Daqaq, "A graphical approach to input-shaping control design for container cranes with hoist," *IEEE Trans. Control Syst. Technol.*, vol. 14, no. 6, pp. 1070–1077, Nov. 2006.

[3] S. Garrido, M. Abderrahim, A. Gimenez, R. Diez, and C. Balaguer, "Anti-swinging input shaping control of an automatic construction crane," *IEEE Trans. Autom. Sci. Eng.*, vol. 5, no. 3, pp. 549–557, Jul. 2008.

[4] W. E. Singhose and J. Vaughan, "Reducing vibration by digital filtering and input shaping," *IEEE Trans. Control Syst. Technol.*, vol. 19, no. 6, pp. 1410–1420, Nov. 2011.

[5] S. Arabasi and Z. Masoud, "Simultaneous travel and hoist maneuver input shaping control using frequency modulation," *Shock Vibrat.*, vol. 2017, pp. 1–12, Jun. 2017.

[6] H. Chen, Y. Fang, and N. Sun, "A swing constraint guaranteed MPC algorithm for underactuated overhead cranes," *IEEE/ASME Trans. Mechatronics*, vol. 21, no. 5, pp. 2543–2555, Oct. 2016.

[7] Z. Wu, X. Xia, and B. Zhu, "Model predictive control for improving operational efficiency of overhead cranes," *Nonlinear Dyn.*, vol. 79, no. 4, pp. 2639–2657, 2015.

[8] H. Chen and N. Sun, "An output feedback approach for regulation of 5-DOF offshore cranes with ship yaw and roll perturbations," *IEEE Trans. Ind. Electron.*, early access, Feb. 2, 2021, doi: 10.1109/TIE.2021.3055159.

[9] X. Wu and X. He, "Nonlinear energy-based regulation control of three-dimensional overhead cranes," *IEEE Trans. Autom. Sci. Eng.*, vol. 14, no. 2, pp. 1297–1308, Apr. 2017.

[10] Y. Fang, B. Ma, P. Wang, and X. Zhang, "A motion planning-based adaptive control method for an underactuated crane system," *IEEE Trans. Control Syst. Technol.*, vol. 20, no. 1, pp. 241–248, Jan. 2012.

[11] Y. Zhao and H. Gao, "Fuzzy-model-based control of an overhead crane with input delay and actuator saturation," *IEEE Trans. Fuzzy Syst.*, vol. 20, no. 1, pp. 181–186, Feb. 2012.

[12] D. Wang, H. He, and D. Liu, "Intelligent optimal control with critic learning for a nonlinear overhead crane system," *IEEE Trans. Ind. Informat.*, vol. 14, no. 7, pp. 2932–2940, Jul. 2018.

[13] H. Ouyang, J. Wang, G. Zhang, L. Mei, and X. Deng, "Novel adaptive hierarchical sliding mode control for trajectory tracking and load sway rejection in double-pendulum overhead cranes," *IEEE Access*, vol. 7, pp. 10353–10361, 2019.

[14] D. Chwa, "Sliding-mode-control-based robust finite-time antisway tracking control of 3-D overhead cranes," *IEEE Trans. Ind. Electron.*, vol. 64, no. 8, pp. 6775–6784, Aug. 2017.

[15] H. Ouyang, J. Hu, G. Zhang, L. Mei, and X. Deng, "Sliding-mode-based trajectory tracking and load sway suppression control for double-pendulum overhead cranes," *IEEE Access*, vol. 7, pp. 4371–4379, 2019.

[16] M. S. Park, D. Chwa, and M. Eom, "Adaptive sliding-mode antisway control of uncertain overhead cranes with high-speed hoisting motion," *IEEE Trans. Fuzzy Syst.*, vol. 22, no. 5, pp. 1262–1271, Oct. 2014.

[17] H. Chen and N. Sun, "Nonlinear control of underactuated systems subject to both actuated and unactuated state constraints with experimental verification," *IEEE Trans. Ind. Electron.*, vol. 67, no. 9, pp. 7702–7714, Oct. 2019.

[18] N. Sun, Y. Wu, X. Liang, and Y. Fang, "Nonlinear stable transportation control for double-pendulum shipboard cranes with ship-motion-induced disturbances," *IEEE Trans. Ind. Electron.*, vol. 66, no. 12, pp. 9467–9479, Dec. 2019.

[19] N. Sun, Y. Fang, H. Chen, and B. Lu, "Amplitude-saturated nonlinear output feedback antiswing control for underactuated cranes with double-pendulum cargo dynamics," *IEEE Trans. Ind. Electron.*, vol. 64, no. 3, pp. 2135–2146, Mar. 2017.

[20] D. Chwa, "Nonlinear tracking control of 3-D overhead cranes against the initial swing angle and the variation of payload weight," *IEEE Trans. Control Syst. Technol.*, vol. 17, no. 4, pp. 876–883, Jul. 2009.

[21] H. I. Jaafar and Z. Mohamed, "PSO-tuned PID controller for a nonlinear double-pendulum crane system," in *Proc. 17th Asia Simul. Conf.*, 2017, pp. 203–215.

[22] K. Zavari, G. Pipeleers, and J. Swevers, "Gain-scheduled controller design: Illustration on an overhead crane," *IEEE Trans. Ind. Electron.*, vol. 61, no. 7, pp. 3713–3718, Jul. 2014.

[23] T. Yang, N. Sun, and Y. Fang, "Adaptive fuzzy control for a class of MIMO underactuated systems with plant uncertainties and actuator deadzones: Design and experiments," *IEEE Trans. Cybern.*, early access, Feb. 2, 2021, doi: 10.1109/TCYB.2021.3050475.

[24] T. Yang, N. Sun, H. Chen, and Y. Fang, "Observer-based nonlinear control for tower cranes suffering from uncertain friction and actuator constraints with experimental verification," *IEEE Trans. Ind. Electron.*, vol. 68, no. 7, pp. 6192–6204, Jul. 2021.

[25] B. Kiss and N. Wang, "Robust exact linearization of a 2D overhead crane," in *Proc. 12th IFAC Symp. Robot Control*, 2018, vol. 51, no. 22, pp. 354–359.

[26] B. Kiss, J. Lévine, and P. Mullhaupt, "Modeling, flatness and simulation of a class of cranes," *Periodica Polytechnica-Elect. Eng.*, vol. 43, no. 3, pp. 215–225, 1999.

[27] M. Fliess, J. Lévine, and P. Rouchon, "A generalized state variable representation for a simplified crane description," *Int. J. Control*, vol. 58, no. 2, pp. 277–283, Aug. 1993.

[28] J. Lévine, P. Rouchon, G. Yuan, C. Grebogi, B. R. Hunt, E. Kostelich, E. Ott, and J. Yorke, "On the control of US Navy cranes," in *Proc. Eur. Control Conf.*, Jul. 1997, p. N-217.

[29] T. Rózsa and B. Kiss, "Tracking control for two-dimensional overhead crane: Feedback linearization with linear observer," in *Proc. 8th Int. Conf. Inform. Control, Automat., Robot.*, 2011, pp. 427–432.

[30] H. Chen, Y. Fang, and N. Sun, "Optimal trajectory planning and tracking control method for overhead cranes," *IET Control Theory Appl.*, vol. 10, no. 6, pp. 692–699, Apr. 2016.

[31] M. Ebrahimi, M. Ghayour, S. M. Madani, and A. Khoobroo, "Swing angle estimation for anti-sway overhead crane control using load cell," *Int. J. Control, Autom. Syst.*, vol. 9, no. 2, pp. 301–309, Apr. 2011.

[32] F. Rauscher, S. Nann, and O. Sawodny, "Motion control of an overhead crane using a wireless hook mounted IMU," in *Proc. Annu. Amer. Control Conf. (ACC)*, Jun. 2018, pp. 5677–5682.

[33] U. Schaper, C. Sagert, O. Sawodny, and K. Schneider, "A load position observer for cranes with gyroscope measurements," *IFAC Proc. Volumes*, vol. 44, no. 1, pp. 3563–3568, 2011.

[34] F. Xing-Yu, N. Dan, L. Qi, and L. Jin-Bo, "Position-pose measurement of crane sway based on monocular vision," *J. Eng.*, vol. 2019, no. 22, pp. 8330–8334, Nov. 2019.

[35] L.-H. Lee, C.-H. Huang, S.-C. Ku, Z.-H. Yang, and C.-Y. Chang, "Efficient visual feedback method to control a three-dimensional overhead crane," *IEEE Trans. Ind. Electron.*, vol. 61, no. 8, pp. 4073–4083, Aug. 2014.

[36] X. Wu, K. Xu, and X. He, "Disturbance-observer-based nonlinear control for overhead cranes subject to uncertain disturbances," *Mech. Syst. Signal Process.*, vol. 139, May 2020, Art. no. 106631.

[37] H. Moradi and G. Vossoughi, "State estimation, positioning and anti-swing robust control of traveling crane-lifter system," *Appl. Math. Model.*, vol. 39, no. 22, pp. 6990–7007, Nov. 2015.

[38] Y. Qian and Y. Fang, "Switching logic-based nonlinear feedback control of offshore ship-mounted tower cranes: A disturbance observer-based approach," *IEEE Trans. Autom. Sci. Eng.*, vol. 16, no. 3, pp. 1125–1136, Jul. 2019.

[39] Z. Zhang, L. Li, and Y. Wu, "Disturbance-observer-based antiswing control of underactuated crane systems via terminal sliding mode," *IET Control Theory Appl.*, vol. 12, no. 18, pp. 2588–2594, Dec. 2018.

[40] C. Hu, W. Chen, Y. Chen, and D. Liu, "Adaptive Kalman filtering for vehicle navigation," *J. Global Positioning Syst.*, vol. 2, no. 1, pp. 42–47, Nov. 2003.

[41] C. H. Kang, S. Y. Kim, and C. G. Park, "Global navigation satellite system interference tracking and mitigation based on an adaptive fading Kalman filter," *IET Radar, Sonar Navigat.*, vol. 9, no. 8, pp. 1030–1039, Oct. 2015.

[42] B. Zheng, P. Fu, B. Li, and X. Yuan, "A robust adaptive unscented Kalman filter for nonlinear estimation with uncertain noise covariance," *Sensors*, vol. 18, no. 3, p. 808, Mar. 2018.

[43] Y. Huang, Y. Zhang, Z. Wu, N. Li, and J. Chambers, "A novel adaptive Kalman filter with inaccurate process and measurement noise covariance matrices," *IEEE Trans. Autom. Control*, vol. 63, no. 2, pp. 594–601, Feb. 2018.

[44] A. H. Mohamed and K. P. Schwarz, "Adaptive Kalman filtering for INS/GPS," *J. Geodesy*, vol. 73, no. 4, pp. 193–203, 1999.

[45] J. Kim, D. Lee, B. Kiss, and D. Kim, "An adaptive unscented Kalman filter with selective scaling (AUKF-SS) for overhead cranes," *IEEE Trans. Ind. Electron.*, vol. 68, no. 7, pp. 6131–6140, Jul. 2021.

[46] J. Lévine, *Analysis and Control of Nonlinear Systems: A Flatness-based Approach*. New York, NY, USA: Springer, 2009.

[47] J. A. Farrell and M. M. Polycarpou, *Adaptive Approximation Based Control: Unifying Neural Fuzzy and Traditional Adaptive Approximation Approaches*. Hoboken, NJ, USA: Wiley, 2006.

[48] H. K. Khalil, *Nonlinear Systems*, 2nd ed. Upper Saddle River, NJ, USA: Prentice-Hall, 1996.

[49] A. F. Lynch and S. A. Bortoff, "Nonlinear observers with approximately linear error dynamics: The multivariable case," *IEEE Trans. Autom. Control*, vol. 46, no. 6, pp. 927–932, Jun. 2001.

[50] S. Sarkka, "On unscented Kalman filtering for state estimation of continuous-time nonlinear systems," *IEEE Trans. Autom. Control*, vol. 52, no. 9, pp. 1631–1641, Sep. 2007.

[51] M. Takeno and T. Katayama, "A numerical method for continuous-discrete unscented Kalman filter," *Int. J. Innov. Comput. Inf. Control*, vol. 8, no. 3, pp. 2261–2274, 2012.

[52] E. A. Wan and R. Van Der Menwe, "The unscented Kalman filter for nonlinear estimation," in *Proc. Symp. Adapt. Syst. Signal Process., Commun. Contr.*, 2000, pp. 153–158.

[53] Y. Zhao, B. Liang, and S. Iwnicki, "Friction coefficient estimation using an unscented Kalman filter," *Vehicle Syst. Dyn.*, vol. 52, no. 1, pp. 220–234, May 2014.

[54] S. Julier, J. Uhlmann, and H. F. Durrant-Whyte, "A new method for the nonlinear transformation of means and covariances in nonlinear filters," *IEEE Trans. Autom. Control*, vol. 45, no. 3, pp. 477–482, Mar. 2000.

[55] R. L. Williams, "Simplified robotics joint-space trajectory generation with a via point using a single polynomial," *J. Robot.*, vol. 2013, pp. 1–6, Feb. 2013.

DONGGIL KIM received the B.Sc., M.Sc., and Ph.D. degrees in electronics engineering from Kyungpook National University, Daegu, South Korea, in 2006, 2008, and 2015, respectively. From 2015 to 2017, he was a Senior Researcher with the Defense Agency for Technology and Quality, South Korea. Since 2017, he has been with the Department of Robot Engineering, Kyungil University, Gyeongsan, South Korea, where he is currently an Assistant Professor. His current research interests include fault tolerant control, fault detection and diagnosis, and fieldbus for the design of dependable networked control systems.

JAEHOON KIM received the B.S. and M.S. degrees in electronics engineering, and the Ph.D. degree in electronic and electrical engineering from Kyungpook National University, Daegu, South Korea, in 2011, 2013, and 2021, respectively. In 2020, he served as a Lecturer with the College of Information and Communication Engineering, Daegu University, Gyeongsan, South Korea. He is currently a Postdoctoral Research Fellow with the Center for ICT and Automotive Convergence, Kyungpook National University. His current research interests include non-linear estimation and filtering, control engineering, and monitoring and diagnostic techniques.

BÁLINT KISS (Member, IEEE) received the M.S. degree in electrical engineering from Budapest University of Technology and Economics (BME), Hungary, in 1996, followed by a DEA at Université Paris XI, in 1997, and the Ph.D. degree from the Ecole des Mines de Paris, France, in 2001. He is currently an Associate Professor with the Department of Control Engineering and Information Technology, BME. His research interests include control of mechatronic systems and robotics.

DONGIK LEE (Member, IEEE) received the B.S. and M.S. degrees in control engineering from Kyungpook National University, Daegu, South Korea, in 1987 and 1990, respectively, and the Ph.D. degree in complex systems control engineering from Sheffield University, Sheffield, U.K., in 2002.

He is currently a Professor with the School of Electronic and Electrical Engineering, Kyungpook National University. His research interests include design of real-time networked control for various safety-critical applications, including autonomous underwater vehicles, wind turbines, and intelligent automobiles.

● ● ●